Journal of Controlled Release 272 (2018) 62–71

Contents lists available at ScienceDirect

Journal of Controlled Release

journal homepage: www.elsevier.com/locate/jconrel

Fate of PEGylated antibody fragments following delivery to the lungs: Influence of delivery site, PEG size and lung inflammation

Harshad P. Patil[a,1], Danielle Freches[a], Linda Karmani[b], Gregg A. Duncan[c,d,2], Bernard Ucakar[a], Jung Soo Suk[c,d], Justin Hanes[c,d,e], Bernard Gallez[b], Rita Vanbever[a,*]

[a] Advanced Drug Delivery & Biomaterials, Louvain Drug Research Institute, Université catholique de Louvain, Brussels, Belgium
[b] Biomedical Magnetic Resonance Group, Louvain Drug Research Institute, Université catholique de Louvain, Brussels, Belgium
[c] Center for Nanomedicine, Wilmer Eye Institute, Johns Hopkins University School of Medicine, Baltimore, USA
[d] Department of Ophthalmology, Wilmer Eye Institute, Johns Hopkins University School of Medicine, Baltimore, USA
[e] Department of Biomedical, Chemical and Biomolecular Engineering, Johns Hopkins University, Baltimore, USA

ARTICLE INFO

Keywords:
Polyethylene glycol
Anti-IL-17A
Anti-IL-13
Lung periphery
Central airways
Residence time
Mucus
Lung inflammation

ABSTRACT

Pulmonary administration of anti-cytokine antibodies offers a targeted therapy in asthma. However, the rapid elimination of proteins from the lungs limits the efficacy of inhaled medications. PEGylation has been shown to increase the residence time of anti-interleukin (IL)-17A and anti-IL-13 antibody fragments in the lungs and to improve their therapeutic efficacy. Yet, little is known about the factors that affect the residence time of PEGylated antibody fragments in the lungs following pulmonary delivery. In this study, we showed that the molecular weight of polyethylene glycol (PEG), 20 kDa or 40 kDa, had a moderate effect on the residence time of an anti-IL-17A Fab′ fragment in the lungs of mice. By contrast, the site of delivery of the anti-IL-17A and anti-IL-13 Fab′ fragments within the lungs had a major impact on their residence time, with the deeper the delivery, the more prolonged the residence time. The nature of the Fab′ fragment had an influence on its residence time as well and the anti-IL-17A Fab′ benefited more from PEGylation than the anti-IL-13 Fab′ did. Acute lung inflammation slightly shortened the residence time of the anti-IL-17A and anti-IL-13 Fab′ fragments in the lungs but PEGylation was able to prolong their presence in both the healthy and inflamed lungs. Antibody fragments were predominately located within the airway lumen rather than the lung parenchyma. Transport experiments on monolayers of Calu-3 cells and studies of fluorescence recovery after photobleaching in respiratory mucus showed that mechanisms involved in the prolonged presence of PEGylated Fab′ in the airway lumen might include binding to the mucus, reduced uptake by respiratory cells and reduced transport across lung epithelia. Finally, using I^{125}-labeled anti-IL-17A Fab′, we showed that the protein fragment hardly penetrated into the lungs following subcutaneous injection, as opposed to pulmonary delivery.

1. Introduction

Asthma is a disorder of the conducting airways that is characterized by acute or chronic airways inflammation, mucus production and airway hyperresponsiveness resulting in airway remodeling [1]. It is estimated that approximately 10% of the population suffer from asthma and in Europe alone the total cost of asthma treatment is around 17.7 billion Euro [2]. Asthma results from combination effects of cells of the innate and adaptive immune systems together with epithelial cells [1]. Various Th1 cytokines like interferon γ, Th-2 cytokines like IL-4, IL-5, IL-9, IL-13 and Th-17 cytokine like IL-17 are released in the lungs and their complex coordination induces asthma [1].

Abbreviations: BAL, bronchoalveolar lavage; DMEM, Dulbecco's Modified Eagle Medium; EDTA, ethylenediaminetetraacetic acid; ELISA, enzyme-linked immunosorbent assay; ET, endotracheal; FRAP, fluorescence recovery after photobleaching; HBSS, Hank's balanced salt solution; I^{125}, Iodine-125; IL, interleukin; LPS, lipopolysaccharide; mAb, monoclonal antibody; MW, molecular weight; NAL, nasal lavage; PBS, phosphate buffer saline; PEG, polyethylene glycol; PEG20, linear 20 kDa polyethylene glycol; PEG40, two-armed 40 kDa polyethylene glycol; SC, subcutaneous; SDS-PAGE, sodium dodecyl sulfate polyacrylamide gel electrophoresis; SEM, standard error of the mean; Th, T helper; TEER, transepithelial electrical resistance; τ_{mucus}, time to 50% recovery in mucus

* Corresponding author at: Université catholique de Louvain, Louvain Drug Research Institute, Advanced Drug Delivery and Biomaterials, Avenue Emmanuel Mounier 73, Brussels 1200, Belgium.
E-mail address: rita.vanbever@uclouvain.be (R. Vanbever).
[1] Present address: Department of Communicable Diseases, Interactive Research School for Health Affairs, Bharati Vidyapeeth University, Pune, Maharashtra, India.
[2] Present address: Fischell Department of Bioengineering, University of Maryland, College Park, USA.

https://doi.org/10.1016/j.jconrel.2017.12.009
Received 5 October 2017; Received in revised form 11 December 2017; Accepted 13 December 2017
Available online 13 December 2017
0168-3659/

Cytokines play an important role in modulating and maintaining inflammation in asthma. Thus, blocking cytokines might help to decrease inflammation and reduce severity of the disease. Unlike chemical drugs, monoclonal antibodies (mAbs) offer a highly targeted therapy owing to their ability to only bind to their specific targets. In line with this, many mAbs against various cytokines like IL-4, IL-5, IL-13, IL-9, IL-17 and tumor necrosis factor alpha are clinically investigated and some are approved for clinical use [3].

Currently, all the clinically approved mAbs for cytokine inhibition in asthma are delivered by injection. However, mAb concentration in the lungs is significantly lower after parenteral delivery than after pulmonary delivery [4]. This effect might be due to poor rate of convective and diffusional transport [5]. Moreover, systemic delivery of the mAb does not rule out the possibility of systemic side effects such as serum sickness or cytokine release syndrome which make delivery of the mAb directly to the lungs an attractive alternative [6].

Inhalation of mAbs offers topical delivery to the lungs and reduces systemic exposure, thus limiting side effects in secondary organs. However, factors like mucociliary clearance, uptake of mAbs by alveolar macrophages, pulmonary metabolism and the large alveolar membrane that results in transport of macromolecules to the bloodstream might limit the efficacy of inhaled mAbs. Mucociliary action is the predominant mechanism for clearing foreign particulate matter in upper airways. On the other hand, alveolar macrophages and the large alveolar membrane cause non-availability of mAbs to perform their function in the alveolar region [7].

PEGylation is thought to improve the residence time of antibody fragments in the lungs through mucoadhesion and reduced uptake of PEG-mAb conjugates by alveolar macrophages [8]. Compared to biodegradable microspheres, drug conjugation to PEG allows increased protein loading and maximization of the inhalation dose [9]. An increase in the molecular weight (MW) of PEG has been shown to prolong the residence time of the free polymer in the airway lumen [10]. In line with this, PEGylation of proteins with a PEG chain of increasing size decreased the systemic bioavailability of the proteins following intratracheal instillation in rats, suggesting their increased retention within the lungs [11]. Conjugation of a two-armed 40 kDa PEG chain to anti-IL-17A $F(ab')_2$ and anti-IL-13 Fab′ greatly prolonged the presence of these fragments within the lungs of mice and reduced house dust mite-induced lung inflammation [8]. Therefore, PEG size and architecture could affect residence of mAb in the luminal side of the lungs and affect its diffusion to the parenchyma. In addition, two-armed 40 kDa PEG is more effective in protecting the conjugated protein from degradation by enzymes than a single linear 20 kDa PEG [12]. Proteins modified with two-armed PEG retain more activity as compared to the same protein modified with several small linear PEGs [13]. The delivery site within the lungs could also affect the residence of PEGylated proteins within the lungs [14]. Mucus thickness, type of epithelial and phagocytic cells and proteases might affect the residence of PEGylated mAbs.

In this article, we investigated factors that affected the residence time of PEGylated Fab′ antibody fragments in the lungs: PEG size, site of delivery within the respiratory tract, nature of the antibody fragment, lung inflammation. Linear 20 kDa PEG and two-armed 40 kDa PEG were selected for our study based on large MW PEGs already used clinically [15]. In addition, the clearance mechanisms of antibody fragments from the lungs were investigated through transport and uptake experiments in monolayers of Calu-3 cells, a bronchial epithelial cell line, diffusion measurements in human airway mucus and biodistribution studies of radiolabeled Fab′ in mice.

2. Materials and methods

2.1. PEGylation of Fab′

Anti-IL-13, anti-IL-13-PEG40 and anti-IL-17A Fab′ were kindly provided by UCB Pharma (Slough, United Kingdom). Site-specific PEGylation of anti-IL-17A Fab′ was carried out by using linear 20 kDa PEG-maleimide (PEG20) or two-armed 40 kDa PEG-maleimide (PEG40; NOF Corporation, Tokyo, Japan) [16,17]. Briefly, anti-IL-17A Fab′ was reduced by diafiltration (Amicon 8010 stirred cells with 10,000 MWCO; Merck Millipore, Overijse) against 1 mM β-mercaptoethylamine (Sigma, Diegem, Belgium) in 0.1 M sodium phosphate buffer, 2 mM ethylenediaminetetraacetic acid (EDTA), pH 5.9 at room temperature for 8 h. Reduction generated a free thiol group at the hinge region of the Fab′ to which PEG-maleimide was attached. The reduction used 8 equivalent sample volumes. β-mercaptoethylamine was removed from the sample by running > 7 equivalent sample volumes of 0.1 M sodium phosphate buffer, 2 mM EDTA, pH 5.9 at room T° for 8 h. The reduced Fab′ solution was mixed with PEG maleimide at a molar ratio of 1:1.2 (Fab′:PEG) in 0.1 M sodium phosphate buffer, 2 mM EDTA, pH 5.9 and left at room temperature under agitation overnight. The solution was then dialyzed against 20 mM succinic acid, 5 mM NaCl, pH 4.6 (buffer A) prior to purification by cation-exchange chromatography (Resource S, 6 ml column, GE Healthcare Bio-Sciences AB) on an ÄKTA™ purifier 10 system (GE Healthcare Bio-Sciences AB). A salt gradient elution was used. Buffer A was 20 mM succinic acid, 5 mM NaCl, pH 4.6 and buffer B was 20 mM succinic acid, 350 mM NaCl, pH 4.6. Collected fractions were analyzed for multi-PEGylated, mono-PEGylated and non-PEGylated Fab′ by sodium dodecyl sulfate polyacrylamide gel electrophoresis (SDS-PAGE) using gradient 4–20% Mini-PROTEAN®TGXTM precast gel (Bio-Rad), as described previously [17]. Fractions containing mono-PEGylated Fab′ were pooled and concentrated using Vivaspin 15R sample concentrator (Sartorius; Stonehouse, Gloucestershire, UK). Concentrated PEGylated Fab′ was reconstituted in 2 mM EDTA, 0.1 M sodium phosphate buffer pH 5.9 and stored at 4 °C until used. Successful mono-PEGylation of the anti-IL17A Fab′ was previously demonstrated by our laboratory using SDS-PAGE and matrix-assisted laser desorption/ionization time-of-flight mass spectrometry [17].

2.2. Radiolabeling of Fab′

Radiolabeling of anti-IL-17A, anti-IL-17A-PEG20 and anti-IL-17A-PEG40 Fab′ was carried out with Iodine-125 (I^{125}; Perkin Elmer, Zaventem, Belgium). Protocol for direct iodination was followed using Pierce™ pre-coated iodination tubes (Thermo Scientific, Gent, Belgium) as per manufacturer suggestions with few modifications. Briefly, Fab′ fragments were diluted to a concentration of 1 mg/ml using phosphate buffer saline (PBS), pH 7.4 and 100 μl were added to pre-coated iodination tubes. Then, 250 μCi of I^{125} was added to the Fab′ in pre-coated tubes and the reaction was allowed to proceed under mild agitation for 25 min. The reaction was terminated by removing the reaction mixture from the tubes and PBS was added to reach a volume of 1 ml. Free iodine was removed using Sephadex gel filtration columns and PBS as elution buffer. The radiochemical purity was evaluated by thin layer chromatography. SDS-PAGE analysis of antibody fragments was performed to evaluate the protein integrity following the direct iodination procedure.

2.3. Animals

Animal experiments were approved by the Institutional Animal Care and Use Committee of the Université catholique de Louvain (Permit number: 2012/UCL/MD/006). In vivo experiments were performed in 7–8 week old female NMRI mice (Elevage Janvier, Le Genest-St-Isle, France).

Mice (n = 5 to 6 per experimental group) were anesthetized using ketamine/xylazine (90/10 mg/kg). To determine the impact of the delivery site on pulmonary residence time in healthy mice, 10 μg of non-PEGylated or PEGylated Fab′ were delivered to the deep lung or to central airways, as previously described [14]. Briefly, a laryngoscope

(Penn-Century Inc., Philadelphia, USA) was used to correctly place the bended and blunt needle of a 100 μl precision micro-syringe (Hamilton, Bonaduz, Switzerland) into the trachea. For deep lung delivery, mice were placed on their back with a tilt angle of 45°. Twenty-five μl of solution containing 10 μg Fab′ were delivered followed by a 200 μl air bolus using 1 ml syringe having an angled 18 gauge needle with a blunt tip. For central airway delivery, mice were placed on their back and 10 μl of solution containing 10 μg Fab′ fragments was delivered slowly and no air bolus was insufflated. PEG was not counted in the mass delivered and recovered from the respiratory tract. Therefore, the different mouse groups received the same number of moles of mAb fragments, that is, 0.21 nmol. At pre-determined times following antibody delivery (immediately, 4 h, 24 h or 48 h), anesthetized mice were sacrificed by cervical dislocation and nasal lavage (NAL), bronchoalveolar lavage (BAL) and lungs were collected. All the samples from mice administered with anti-IL-13 or anti-IL-17A and anti-IL-17A-PEG20 were collected in PBS containing complete protease inhibitor cocktail (Roche, Almere, The Netherlands). On the other hand, samples from mice administered with anti-IL-13-PEG40 or anti-IL-17A-PEG40 were collected using PBS containing complete protease inhibitor cocktail with 0.1% triton. Triton increases recovery of PEG40-proteins from biological samples whereas it does not for PEG20-proteins or even slightly decreases recovery for non-PEGylated proteins [8]. The nasal lavage was performed by cannulating the trachea toward the nasal cavity and instilling 1 ml of PBS. The fluid emerging from the nostrils was collected. The BAL was collected by flushing the luminal side of the lungs through the trachea with 1 ml PBS three times. The resected lungs were homogenized in 1 ml PBS using a tissue grinder (Polytron; Kinematica, Luzern, Switzerland). All the samples were centrifuged at 5000 rpm and 4 °C for 10 min. The supernatants were collected and stored at − 20 °C until analysis.

The residence time of non-PEGylated or PEGylated anti-IL-17A Fab′ in the inflamed lungs was studied by inducing lung inflammation with lipopolysaccharide (LPS). Ten micrograms of LPS from *Escherichia coli* (Sigma-Aldrich, Saint Louis, USA) in 50 μl PBS were instilled intranasally (25 μl per nostril) [18]. Twenty-four hours after LPS delivery, mice received 10 μg of antibodies in their deep lungs and samples were collected as described above.

For biodistribution studies, 10 μg of non-PEGylated or PEGylated anti-IL-17A I^{125}-radiolabeled Fab′ corresponding to 1.5 μCi was delivered to the deep lungs of mice (n = 3 to 5), as described above [14]. Similarly, control mice (n = 3) received 1.5 μCi of I^{125} diluted in PBS to the deep lungs. To determine the exact amount of injected dose, the syringe used for deep lung delivery was weighed before and after mAb delivery. To compare pulmonary delivery with systemic delivery, non-PEGylated anti-IL-17A Fab′ was also delivered to mice by subcutaneous injection. Four hours after mAb delivery, blood was collected by retro-orbital puncture under the anesthesia of ketamine/xylazine and mice were sacrificed by cervical dislocation. Nasal lavage, BAL, lungs, thyroid, stomach, small intestine, kidney, urinary bladder were collected and weighed. The radioactivity of these organs was measured using a Cobra II auto gamma counter (Packard, Minnesota, USA).

2.4. Air interface cell culture

Calu-3 cells were used to develop air-interface culture, as described previously with few modifications [19,20]. Cells were cultured in Dulbecco's Modified Eagle Medium (DMEM) with L-glutamine containing 10% fetal bovine serum (v/v), 1 mM sodium pyruvate, 100 units/ml penicillin, 100 μg/ml streptomycin. All supplements were from Gibco (Life Technologies B.V., Gent, Belgium). The cells were maintained in 75 cm^2 cell culture flasks (Cellstar® Tissue culture flasks; Greiner Bio-one, Germany) at 37 °C with 5% CO_2. Medium was changed every alternate day and cells were subcultured when they were 85–90% confluent. For cell subculture, cells were detached using trypsin-EDTA (0.25%/0.03% in PBS) and 1:4 split ratio was maintained.

Calu-3 cells were seeded on the apical side of 1.12 cm^2 surface area Transwell® culture inserts at a density of 10^6 cells in 500 μl (sterile 24 well plates, 0.4 μm pore size; Corning costar; New-York, USA). For each culture insert, 0.5 ml and 1.5 ml of supplemented DMEM was placed in the apical and basolateral sides, respectively. After 24 h, the medium from both the apical and basolateral sides of the Transwell inserts was removed carefully. 500 μl and 1000 μl of Hank's balanced salt solution (HBSS) was added to the apical and basal sides, respectively and transepithelial electrical resistance (TEER) was measured using chopstick electrodes and volt-ohm meter (EVOM2, World Precision Instrument, Sarasota, USA). After removal of HBSS from both the apical and basal sides, cells were nourished by addition of 1 ml of supplemented DMEM to the basal side. The procedure was repeated every alternate day. Resistance of > 400 Ω cm^2 was developed 5 days post seeding. Cells were further maintained for 23 days for complete transformation and mucus secretion [21].

After the development of a sufficient resistance, 10 μl of 1 mg/ml non-PEGylated or PEGylated anti-IL-13 or anti-IL-17A in HBSS were added to the apical side of the cells. At pre-determined times (immediately, 4, 24 or 48 h) following the addition of mAbs, the basolateral medium and the apical surface fluid were collected, the TEER was measured to check integrity of the monolayer and cells were lysed. The basolateral medium was collected directly while the apical surface fluid was obtained by gently washing the apical side of the cells three times with 60 μl chilled HBSS. Cell lysis supernatant was obtained by cells lysis using 100 μl lysis buffer (M-PER Mammalian Protein Extraction Reagent; Thermo-Scientific, Gent, Belgium). Lysed cells were scrapped out of the well using a pipette tip, centrifuged at 5000 rpm at 4 °C for 10 min and the supernatant was collected. Samples were stored at − 20 °C until analysis.

2.5. ELISA

Non-PEGylated or PEGylated anti-IL-13 or anti-IL-17A were analyzed in NAL, BAL, supernatants of lung homogenate and cell culture samples by enzyme-linked immunosorbent assay (ELISA), as previously described [17].

2.6. FRAP

Human airway mucus samples were collected in accordance with a protocol approved by the Johns Hopkins Medicine Institutional Review Board (study #NA_00038606). Informed consent was not required because we collect a surgical waste product (i.e., endotracheal tubes was collected), and all comorbidity data were de-identified, minimizing potential risk to patients. Mucus samples were collected by the endotracheal (ET) tube method. Briefly, patients requiring intubation as part of general anesthesia for elective, non-cardiothoracic surgery at the Johns Hopkins Hospital were identified. Only patients with no respiratory comorbidities and/or smoking history were included in this study. The ET tube was removed from the patient after surgery and the distal end (last ~10 cm portion) was cut and placed in a 50 ml centrifuge tube. Endotracheal tubes were suspended at the top of the 50 ml centrifuge tube using syringe needles and were then spun at 220 × *g* for 30 s. This allowed mucus from the ET tube to collect at the bottom of the 50 ml centrifuge tube and thereafter, the ET tube was disposed. Mucus with visible blood contamination was not included in this study. Mucus samples were stored at 4 °C and analyzed within 24 h of collection.

One hundred micrograms of anti-IL-17A, anti-IL-17A-PEG20 and anti-IL-17A-PEG40 were labeled with FITC using Pierce FITC antibody labeling kit (ThermoFisher Scientific, Gent, Belgium), as per manufacturer protocol. The diffusion of non-PEGylated Fab′ or PEGylated Fab′ in freshly collected human airway mucus samples was determined using fluorescence recovery after photobleaching (FRAP) experiments. 30 μl human airway mucus aliquots were withdrawn using a Wiretrol

(Drummond Scientific Company, Philadelphia, USA) and added to custom microscopy chambers. 0.5 μL of 3–8 mg/ml FITC-labeled Fab′ were added to the 30 μl mucus aliquots and mechanically mixed into the sample with a pipette tip. By adding this small volume, any potential dilution effects on mucus properties can be limited. The chamber was sealed with a small circular coverslip and equilibrated at 4 °C for 1 h before imaging. Samples for FRAP assessment of Fab diffusion in PBS used as a reference were prepared using the same method. FRAP experiments were conducted using a confocal LSM 510 microscope at 63 × magnification with image resolution of 0.28 μm/pixel. A 14 μm × 14 μm rectangular area was rapidly bleached and fluorescence recovery was monitored over a 150 s time period (1.5 s frame rate × 100 total frames). Fluorescence intensity profiles were analyzed using custom MATLAB image processing software that accounts for the effects of photobleaching during the course of experiments to determine the time to 50% recovery in mucus, τ_{mucus}, and mobile fraction of Fab′.

2.7. Statistics

Two way Anova and Tukey or Sidak post-test were performed for comparison of data from groups administered with non-PEGylated vs PEGylated Fab′ fragments. Two-tailed Mann Whitney *U* test was used for comparison of data from groups administered with non-PEGylated vs PEGylated Fab′ when the number of animals within the groups varies. Student's t-test was used for analysis of FRAP experiments. One symbol (#,* or $) means $p < 0.05$, two symbols mean $p < 0.01$ and three symbols mean $p < 0.001$.

3. Results

3.1. Impact of the delivery site and of the PEG size on the residence time of Fab′ fragments in the lungs

Two-armed 40 kDa PEG has been shown effective to increase the residence time of anti-IL-17A F(ab')$_2$ and anti-IL-13 Fab′ mAb fragments in the lungs following intranasal instillation in mice [8]. However, intranasal instillation leads to deposition of the solution within nostrils and upper respiratory airways and might therefore result in rapid mucociliary clearance of the proteins [14]. To assess the impact of the site of delivery within the respiratory tract and of the PEG size on the residence time of mAb fragments, we delivered anti-IL-17A, anti-IL-17A-PEG20 or anti-IL-17A-PEG40 Fab′ to the central airways or to the deep lungs by intratracheal instillation in mice. Quantification of Fab′ fragments in bronchoalveolar lavage (BAL) showed marked reduction of non-PEGylated Fab′ in the airway luminal side 0.25 h post-delivery and complete clearance by 24 h (Fig. 1A and D). In contrast, clearance of the anti-IL-17A-PEG20 and anti-IL-17A-PEG40 was gradual till 48 h. Molecular size of the PEG had no major effect on clearance, except that the anti-IL-17A-PEG40 tended to be cleared from the luminal side of the lungs more gradually than the anti-IL-17A-PEG20 following delivery to the deep lungs (Fig. 1D). Both non-PEGylated and PEGylated Fab′ resided for a longer time in the lumen of the lungs after deep lung delivery than after central airway delivery.

Much lower amounts of Fab′ fragments were detected in the lung tissue compared with the lung luminal side after central airway and deep lung delivery (Fig. 1B and E). Non-PEGylated anti-IL-17A Fab′ was not detected in the lung tissue from 24 h onwards after delivery at both sites. More anti-IL-17A-PEG20 and anti-IL-17A-PEG40 were detected in the lung tissue after deep lung delivery at 0.25 h and 4 h but hardly any effect of PEG molecular size was observed in the residence of the anti-IL-17A-PEG20 and anti-IL-17A-PEG40 at 24 h and 48 h after central airway and deep lung delivery.

Overall, these first results highlight that delivery of antibody fragments to the deep lungs is superior to increase the residence time of the proteins in the lungs than their delivery to central airways (Fig. 1C and F). Moreover, PEGylation is an effective method to enhance the residence time of the Fab′ fragments at both delivery sites and the larger the PEG, the more prolonged the residence time following delivery to the deep lungs.

3.2. Impact of the nature of the antibody fragment on the residence time of Fab′ fragments in the lungs

To confirm the data obtained with the anti-IL-17A Fab′, the residence time of anti-IL-13 Fab′ fragments in the lungs was assessed (Fig. 2). Different Fab′ fragments have different protein primary structures and might therefore present a different sensitivity toward proteolysis and other elimination pathways. As seen from Fig. 2, the nature of the Fab′ fragment had an impact on its residence time in the lungs. The amounts of anti-IL-13 and anti-IL-13-PEG40 recovered from the lungs were closer to each other than they were in the case of the anti-IL-17A and anti-IL-17A-PEG40 (Fig. 1). This was especially the case after delivery of the anti-IL-13 Fab′ fragments to the deep lungs where only a slight but non-significant effect of PEGylation on the residence time of the antibody fragment could be noted (Fig. 2F). However, in line with the anti-IL-17A results, delivery to the deep lungs was superior to increase the residence time of both anti-IL-13 and anti-IL-13-PEG40 than delivery to central airways. In addition, PEGylation greatly increased the residence time of the anti-IL-13 Fab′ following delivery to central airways (Fig. 2C).

3.3. Impact of lung inflammation on the residence time of Fab′ fragments in the lungs

Asthma is a condition where inflammation occurs in the lungs. Lung inflammation might cause differences in clearance of non-PEGylated and PEGylated Fab′ from the airway lumen. Therefore, to study the residence of Fab′ fragments within the inflamed lungs, lipopolysaccharide (LPS) was administered to mice by intranasal instillation 24 h prior to Fab′ delivery to the deep lungs.

Recovery of the non-PEGylated and PEGylated anti-IL-13 Fab′ fragments from the whole lungs highlighted that PEGylation assisted in increasing the residence time of the antibody fragment in the inflamed lungs (Fig. 3A and B). Quantification of the anti-IL-13 Fab′ in BAL and supernatant of lung homogenate showed that the amounts of the anti-IL-13 Fab′ recovered from 0.25 h to 48 h were 2- to 4-times lower in the inflamed lungs as compared to the normal lungs (Fig. 3A). On the contrary, no strong difference in the clearance rate of the anti-IL-13-PEG40 was found between the inflamed and the normal lungs (Fig. 3B). The amounts of the PEGylated protein recovered were only twice smaller at 24 h and 48 h in the inflamed vs normal lungs.

No difference in clearance of the non PEGylated anti-IL-17A Fab′ was seen at any time point between the inflamed and the normal lungs (Fig. 3C). Although the pattern of clearance was the same in the inflamed and the normal lungs for the anti-IL-17A-PEG40 Fab′, the quantities recovered were lower in the inflamed lungs (Fig. 3D). The amounts of the anti-IL-17A-PEG40 recovered from the inflamed lungs were 1.3- to 2.2-times lower from 0.25 h to 48 h than those recovered from the normal lungs.

These results highlighted that although there was no drastic difference in clearance of the non-PEGylated and PEGylated Fab′ fragments between the healthy and inflamed lungs, PEGylation prolonged the presence of Fab′ fragments in both the normal and inflamed lungs (Fig. 3).

3.4. In vitro transport of Fab′ fragments across monolayers of Calu-3 cells

To understand intrinsic epithelial permeability of non-PEGylated and PEGylated Fab′ fragments through respiratory cells, transport experiments on monolayers of Calu-3 cells were performed. Non-PEGylated or PEGylated anti-IL-13 and anti-IL-17A Fab′ fragments were added to the apical side and transport within cells and to the basolateral

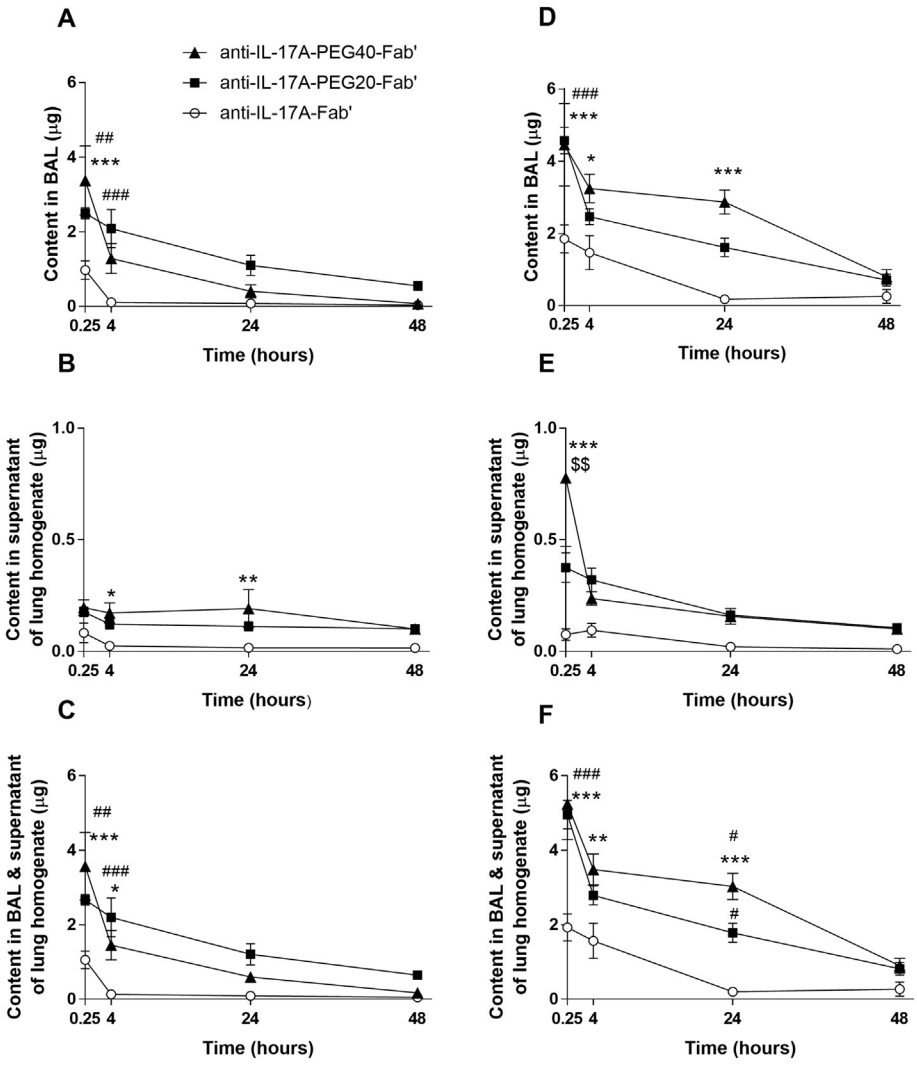

Fig. 1. Impact of the delivery site and of the PEG size on the residence time of Fab′ fragments in the lungs. Quantities of anti-IL-17A, anti-IL-17A-PEG20 and anti-IL-17A-PEG40 recovered from (A, D) bronchoalveolar lavage (BAL), (B, E) supernatant of lung homogenate and (C, F) the combination of BAL and supernatant of lung homogenate following (left panel) central airway or (right panel) deep lung delivery of 10 µg (0.21 nmol) Fab′ fragment per mouse. The PEG is not counted in the mass delivered and recovered from the respiratory tract. The data represent the mean values of 6 mice (± SEM). The data were analyzed using two way ANOVA and Tukey post-test. # represents comparison between anti-IL-17A and anti-IL-17A-PEG20, * represents comparison between anti-IL-17A and anti-IL-17A-PEG40, $ represents comparison between anti-IL-17A-PEG20 and anti-IL-17A-PEG40.

side was analyzed.

Larger amounts of the anti-IL-13-PEG40 stayed on the apical side for 48 h, compared with the non-PEGylated Fab′ (Fig. 4A). About 40% of the non-PEGylated Fab′ was cleared from the apical side by 0.25 h, as opposed to only 6% for the anti-IL-13-PEG40. In line with this, the levels of the anti-IL-13-PEG40 were 1.5-times lower in the cell layers at all times points, compared with the non-PEGylated anti-IL-13 (Fig. 4B). The levels of non-PEGylated Fab′ started increasing in the basolateral medium from 4 h onwards as compared to 24 h for the anti-IL-13-PEG40 (Fig. 4C).

The transport data of the anti-IL-17A Fab′ fragments are in line with those of the anti-IL-13. Forty percent reduction in non-PEGylated anti-IL-17A was observed at the apical side by 0.25 h (Fig. 4D). By comparison, minimal loss of the anti-IL-17A-PEG20 or anti-IL-17A-PEG40 was observed at 0.25 h (Fig. 4D). At later time points, about 1.5 times more anti-IL-17A PEGylated Fab′ than non-PEGylated Fab′ stayed on the apical side. There was 1.5-times lower anti-IL-17A PEG40 Fab′ quantities within the cells and cell layer at all time points than of the anti-IL-17A or anti-IL-17A-PEG20 (Fig. 4E). Surprisingly, no difference was observed between anti-IL-17A Fab′ and anti-IL-17A-PEG20 Fab′ amounts within the cells and cell layer at all time points. Analysis of the basolateral medium highlighted presence of both anti-IL-17A and anti-IL-17A-PEG20 at 4 h while anti-IL-17A-PEG40 was detected only after 24 h. The amount of anti-IL-17A was 2-times higher than that of anti-IL-17A-PEG40 in the basolateral side at 24 h.

Overall, these results indicate that PEG strongly reduces the uptake of Fab′ fragments by cells as well as their transport across the cell monolayer. These effects depended on the PEG size.

3.5. Diffusion of Fab′ fragments in respiratory mucus

To find out whether PEGylation affected Fab′ fragments diffusion through and binding to respiratory mucus, FRAP experiments of anti-IL-17A, anti-IL-17A-PEG20 and anti-IL-17A-PEG40 in normal human respiratory mucus was performed (Fig. 5). Fluorescence recovery after photobleaching showed that non-PEGylated Fab′ diffused at a much faster rate than PEGylated Fab′ in mucus (Fig. 5A). No difference in diffusion rate was observed between anti-IL-17A-PEG20 and anti-IL-17A-PEG40. Time to 50% recovery in mucus normalized by time to 50% recovery in PBS confirmed PEGylated Fab′ diffused more slowly through mucus than non-PEGylated Fab′ (Fig. 5B). The mobile fraction was significantly higher for the non-PEGylated Fab′ than for anti-IL-17A-PEG20 or anti-IL-17A-PEG40 (Fig. 5C), indicating significant binding of the PEGylated Fab′ fragments to the mucus. Similar to diffusion results, no difference in the mobile fraction between the PEGylated fragments was observed.

3.6. Biodistribution of Fab′ fragments in the body following pulmonary delivery

The biodistribution of PEGylated and non-PEGylated Fab′ fragments in the body was compared in mice. I^{125}-labeled anti-IL-17A Fab′, anti-

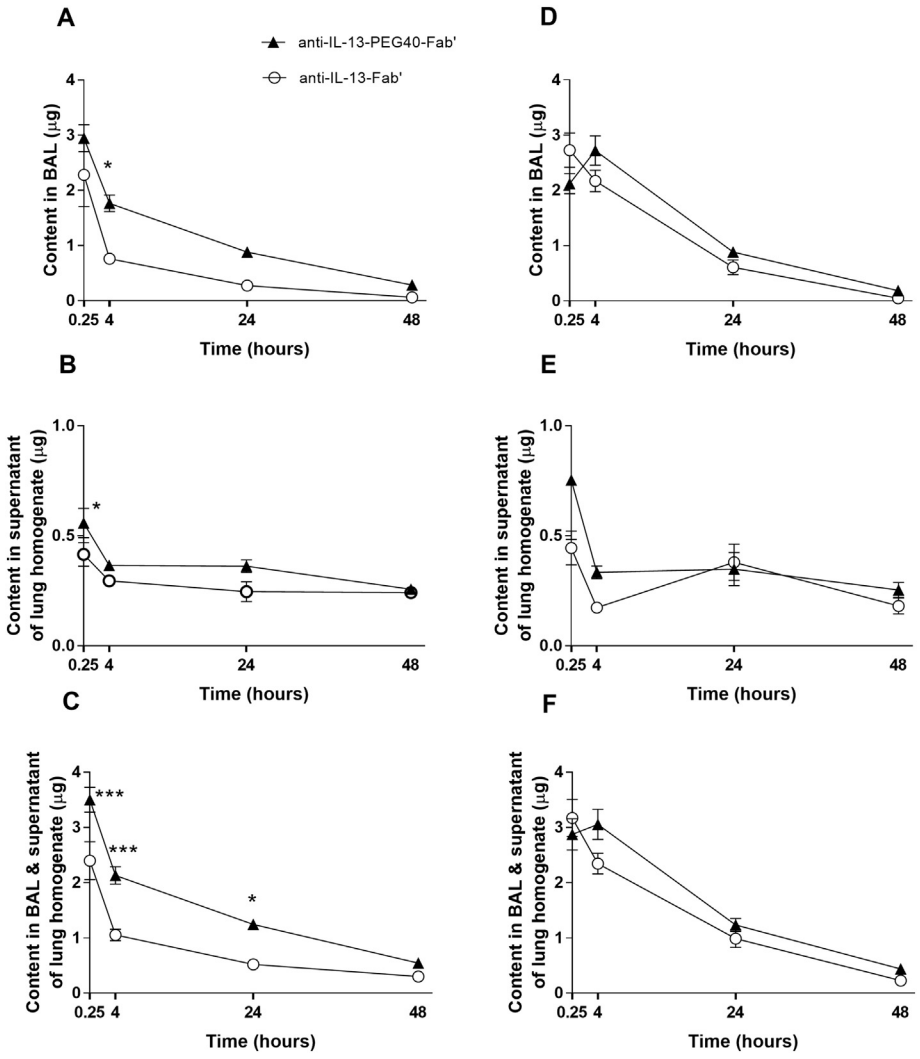

Fig. 2. Impact of the nature of the antibody fragment on its residence time in the lungs. Quantities of anti-IL-13 and anti-IL-13-PEG40 recovered from (A, D) bronchoalveolar lavage (BAL), (B, E) supernatant of lung homogenate and (C, F) the combination of BAL and supernatant of lung homogenate following (left panel) central airway or (right panel) deep lung delivery of 10 μg (0.21 nmol) Fab′ fragment per mouse. The PEG is not counted in the mass delivered and recovered from the respiratory tract. The data represent the mean values of 6 mice (± SEM). The data were analyzed using two way ANOVA and Sidak post-test. * represents comparison between anti-IL-13 and anti-IL-13-PEG40.

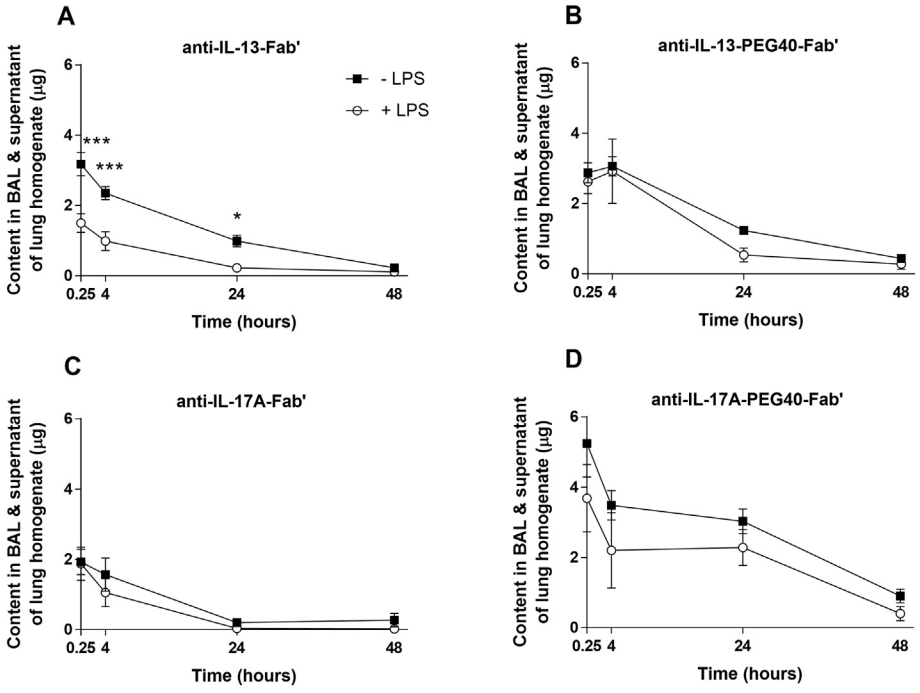

Fig. 3. Impact of lung inflammation on the residence time of Fab′ fragments in the lungs. Quantities of (A) anti-IL-13 and (B) anti-IL-13-PEG40, (C) anti-IL-17A and (D) anti-IL-17A-PEG40 recovered from bronchoalveolar lavage (BAL) and supernatant of lung homogenate following deep lung delivery of 10 μg (0.21 nmol) Fab′ fragment per mouse. The PEG is not counted in the mass delivered and recovered from the respiratory tract. Lung inflammation was induced by intranasal instillation of lipopolysaccharide (LPS) 24 h prior to Fab′ delivery (“ + LPS” groups). The data represent the mean values of 6 mice (± SEM). The data were analyzed using two way ANOVA and Tukey post-test. * represents comparison between healthy (“ − LPS”) and inflamed (“ + LPS”) lungs.

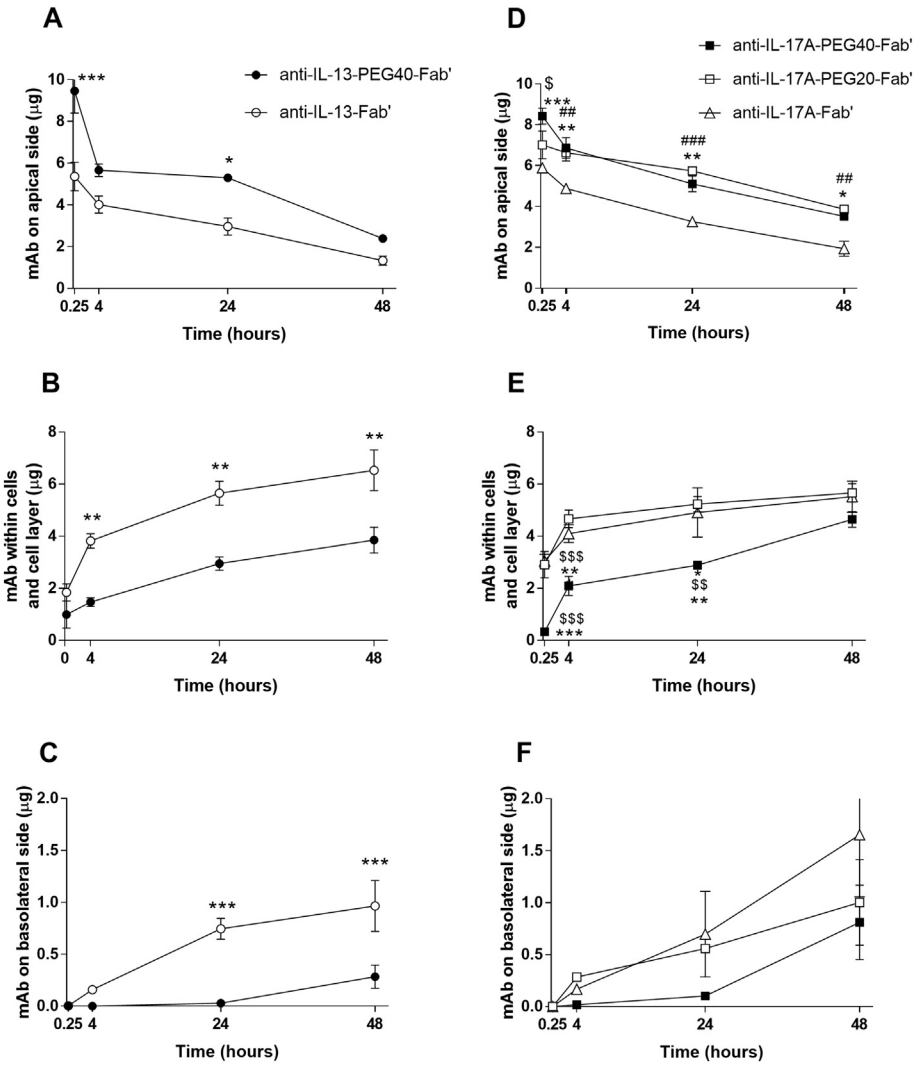

Fig. 4. Transport of (A–C) anti-IL-13 and anti-IL-13-PEG40 and (D–F) anti-IL-17A, anti-IL-17A-PEG20 and anti-IL-17A-PEG40 Fab′ fragments across monolayers of Calu-3 cell grown at an air-interface. 10 μg (0.21 nmol) of Fab′ fragments were added on the apical side of Calu-3 cells and the quantities of Fab′ fragments were quantified in (A, D) the apical surface fluid, (B, E) the cell lysate and (C, F) the basolateral medium. The PEG is not counted in the mass delivered and recovered from the respiratory tract. The data represent the mean values of 3 cell inserts (± SEM). The data were analyzed using two way ANOVA and Tukey post-test. # represents comparison between anti-IL-17A and anti-IL-17-PEG20, * represents comparison between anti-IL-13 (or anti-IL-17A) and anti-IL-13-PEG40 (or anti-IL-17-PEG40), respectively, $ represents comparison between anti-IL-17-PEG20 and anti-IL-17-PEG40.

IL-17A-PEG20 and anti-IL-17A-PEG40 were administered to the deep lungs. To compare pulmonary delivery with systemic delivery, non-PEGylated anti-IL-17A Fab′ was also delivered to mice by the subcutaneous (SC) route. Subcutaneous injection is the most clinically relevant injection route in asthma because patients can easily self-inject medications, without the need for an administration by medical personnel [22]. All mice were sacrificed 4 h after delivery and organs were analyzed for radioactivity content.

Substantial amounts of the instilled dose of the PEGylated and non-PEGylated Fab′ fragments were found in the lungs following deep lung delivery (Fig. 6A). About 16% of the non-PEGylated anti-IL-17, 21% of the anti-IL-17A-PEG20 and 22% of the anti-IL-17A-PEG40 were detected in the BAL (Fig. 6A). By contrast, < 0.05% of the SC-delivered Fab′ reached the BAL. Similarly, 7.6% of the anti-IL-17A, 10% of the anti-IL-17A-PEG20 and 9.5% of the anti-IL-17A-PEG40 were detected in the lung tissue after deep lung delivery. Only 0.3% of the non-PEGylated anti-IL-17A was present in the lung tissue 4 h after SC delivery. Analysis of nasal lavages showed the presence of only small quantities of all the Fab′ fragments following deep lung delivery. In all the mouse groups, a high level of I^{125} radioactivity was detected in the stomach (Fig. 6B). Significantly higher amounts of the anti-IL-17A than of the anti-IL-17A-PEG40 were detected in the stomach following deep lung

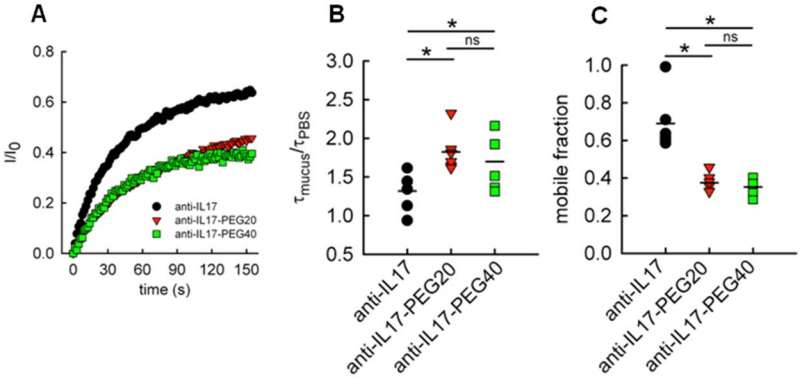

Fig. 5. Diffusion of the anti-IL-17, anti-IL-17A-PEG20 and anti-IL-17A-PEG40 through normal human respiratory mucus. FITC-labeled Fab′ fragments were added to the mucus and diffusion was measured using fluorescence recovery after photobleaching (FRAP). (A) Intensity (I/I0) over time after bleaching at t = 0 s of representative samples, (B) time to 50% recovery in mucus, τ_{mucus}, normalized by time to 50% recovery in PBS, τ_{PBS}, for the anti-IL-17A, anti-IL-17A-PEG20 and anti-IL-17A-PEG40, (C) mobile fraction for the anti-IL-17A, anti-IL-17A-PEG20 and anti-IL-17A-PEG40. The data represent the mean values of 5 different mucus samples (± SEM). A student's *t*-test was used for comparison of the data.

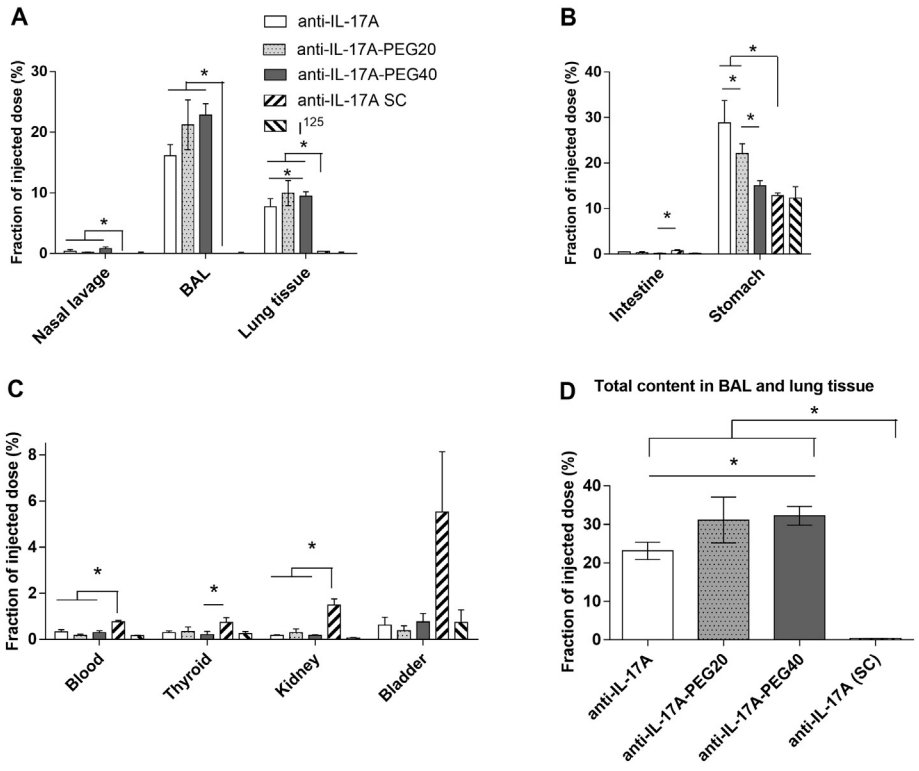

Fig. 6. Biodistribution of Fab′ fragments in different organs following pulmonary delivery. 1.5 μCi of the anti-IL-17A, anti-IL-17A-PEG20 and anti-IL-17A-PEG40 were delivered to each mouse by deep lung delivery and organs were collected 4 h later. Control groups of mice involved deep lung delivery of 1.5 μCi of free I^{125} and subcutaneous (SC) injection of 1.5 μCi of the anti-IL-17A. (A–C) Fraction of the injected dose (%) detected in organs, (D) fraction of the injected dose (%) recovered from the whole lung. The data represent the mean values of 3 to 5 mice per group (± SEM). Two-tailed Mann Whitney *U* test was used for comparison of the data.

delivery. The anti-IL-17A-PEG20 value was intermediated between the anti-IL-17A and anti-IL-17A-PEG40 in the stomach.

In blood samples, the highest quantities of Fab′ fragments were detected after SC delivery (0.7%, Fig. 6C). This amount was three times higher than following deep lung delivery. In the kidney, < 0.2% of the anti-IL-17A delivered to the deep lung were detected while 1.5% was detected after SC injection. Similarly, in the urinary bladder, about 5.5% of the anti-IL-17A was detected 4 h after SC injection. This amount was 9 times higher than the one observed after deep lung delivery. No difference in the quantities of non-PEGylated and PEGylated Fab′ was measured in nasal lavage, blood, thyroid, kidney and urinary bladder following deep lung delivery.

The calculation of the total recovered dose in the whole lung (BAL + lung tissue, Fig. 6D) highlighted that approximately 23% of the anti-IL-17A Fab′ dose, approximately 31% of the anti-IL-17A-PEG20 dose were still detected in the lungs 4 h later. These amounts were approximately 62-, 84- and 86-times higher than the amount obtained following SC injection (0.37%).

4. Discussion

The therapeutic efficacy of a treatment is determined by the availability and the activity of the drug at the site of the disease. In previous studies, we showed that PEG40 increased the residence time of anti-cytokine antibody fragments in the lungs of mice, rats and rabbits and improved their therapeutic efficacy in a murine model of house dust mite-induced lung inflammation [8,17]. Moreover, site-selective attachment of PEG40 to the C-terminal cysteine of an anti-IL-17A Fab′ fragment enhanced nine-fold its intrinsic inhibitory potency [17]. The aim of the present study was to better understand the clearance kinetics of non-PEGylated and PEGylated Fab′ upon delivery to different sites of the lungs as well as their relationship with PEG molecular weight. The biodistribution of Fab′ fragments in different organs was also evaluated after pulmonary delivery and the mechanisms involved in the longer residence time of PEGylated Fab′ in the lungs were clarified.

Similarly to previously published studies [8,17], we found that PEGylation sustained the presence of Fab′ fragments in the lungs. However, the nature of the Fab′ fragment had an impact on its residence time and the anti-IL-17A Fab′ benefited more from PEGylation than the anti-IL-13 Fab′ did. The PEG molecular weight (two-armed 40 kDa PEG vs linear 20 kDa PEG) had a moderate influence on the presence of the anti-IL-17A in the lungs. By contrast, the site of delivery of the Fab′ fragments within the respiratory tract had a large impact on their residence time. Delivery to the lung periphery resulted in a more prolonged residence of both PEGylated and non-PEGylated anti-IL-17A and anti-IL-13 Fab′, compared with delivery to central airways. So, 30% of the delivered dose of the anti-IL-17A-PEG40-Fab′ and 2% of the delivered dose of the anti-IL-17A-Fab′were still present in the lungs 24 h following delivery to the deep lungs. These values were 6 and 1% following delivery to central airways. Many tissue characteristics and clearance pathways differ while descending the respiratory tract [23]. The epithelium is approximately 60 μm thick in the trachea and it progressively thins up to reach a thickness of 0.1 μm to 0.2 μm in the alveolar region. The columnar and ciliated epithelium of the conducting airways is covered by a thick mucus gel while the alveolar epithelium is covered by a thin surfactant lining fluid. The rate of mucociliary clearance exponentially decreases from the proximal airways to the distal airways [24]. The alveolar spaces are populated by alveolar macrophages which continuously take up the surrounding epithelial lining fluid and the compounds present in this fluid [25]. The vast surface area of the alveolar epithelium, the short diffusion path from the alveolar space to the systemic circulation and the dense capillary network can result in a quick systemic absorption of small molecules into the bloodstream. The prolonged presence of the proteins in the lungs following delivery to the deep lungs might result from the reduction in their clearance by the mucociliary escalator. In fact, the mucociliary escalator represents the only clearance pathway which decreases from the upper to the lower airways. Möller et al. targeted ultrafine technetium 99 m-labeled carbon particles to the airways or to the lung periphery in healthy volunteers and similarly showed a prolonged retention of the nanoparticles delivered to the lung periphery [26]. Delivery to the deep lungs in humans can be achieved by adjusting the particle size of the aerosol particles in the desired range of 3 μm [27].

Lung inflammation induced by LPS slightly affected the residence time of Fab′ fragments in the lungs. The amounts of PEGylated and non-PEGylated Fab′ fragments recovered from the inflamed lungs over time were systematically lower compared with those recovered from the normal lungs. However, this reduction was slight and not statistically significant, except for the anti-IL-13-Fab′ which showed a 2- to 4-times reduction in amounts recovered. Intratracheal instillation of LPS induces a massive recruitment of neutrophils into the alveolar spaces and the activation of lung macrophages [18,28]. Degranulation of neutrophils and macrophages releases elastase, cathepsin G, reactive oxygen species and other proteases. The proteases and reactive oxygen species damage the alveolar epithelium and increase its permeability, resulting in protein exudation into the airspaces. Therefore, the slight decrease in Fab′ fragments quantities recovered from the inflamed lungs might come from an increased uptake by phagocytes, an increased proteolysis and/or an increased transport into the systemic circulation. Increased neutrophil recruitment characterize several lung inflammatory conditions in the clinic, in particular, severe asthma, chronic obstructive pulmonary disease, cystic fibrosis, respiratory infections and the acute respiratory distress syndrome. These diseases present additional physiological alterations such as a contraction of conducting airways in asthma and a slow-down mucociliary clearance in cystic fibrosis [1,29]. Nevertheless, these data provide a first idea on how lung inflammation might influence the time of residence of Fab′ fragments in the lungs. Similar results were obtained by Patel et al. using lipid nanocapsules. A 1.5-times lower lung dose of lipid nanocapsules was achieved in LPS-treated mice, compared with saline-treated animals. However, the clearance kinetics of the nanocapsules from the lungs was unaltered by the acute lung inflammation [30].

PEGylation has been shown to prolong the residence time of antibody fragments in the lungs through mucoadhesion and escape from alveolar macrophages rather than increased hydrodynamic size or improved enzymatic stability [8,31]. The FRAP experiments performed in this study support the mucoadhesive character of PEGylated Fab′ fragments which is likely a result of entanglements between the large PEG chains and mucin fibers. In addition, PEGylation of Fab′ increases its hydrodynamic diameter and thereby reduces its diffusion rate. Accordingly, The diffusion of both the anti-IL-17A-PEG20-Fab′ and anti-IL-17A-PEG40-Fab′ through human respiratory mucus was significantly hindered and their mobile fractions significantly reduced compared with the unconjugated anti-IL-17A-Fab′. Moreover, transport experiments on monolayers of Calu-3 cells cultured at an air-interface highlighted that PEGylation sustained the presence of Fab′ fragments at the apical side of the cell monolayer and decreased their cell uptake and transepithelial transport. These observations might be explained by the adhesion of PEGylated Fab′ fragments to the mucin produced by the cells [32]. The decrease in transepithelial transport might also come from the decreased paracellular diffusion of the enlarged conjugated proteins and from the decreased transcytosis reflected in the decreased cell uptake. While PEG40 had a significant effect on apical side residency, cell uptake and transepithelial transport, PEG20 unexpectedly had only an effect on apical side residency and transepithelial transport but not on cell uptake.

Biodistribution studies using I^{125}-labeled Fab′ fragments confirm the efficient targeting of Fab′ fragments to the lung tissue following pulmonary delivery. The BAL and the lung parenchyma contained up to 20 and 10% of the I^{125}-labeled Fab′-delivered dose, respectively. By contrast, only 0.4% of the Fab′ fragment dose reached the lung tissue following SC injection. Seven percent of the SC-injected dose was found in the kidney and bladder, which demonstrates the renal clearance of the systemically-delivered Fab′. Yet, this pathway of clearance was not noticeable following pulmonary delivery. The negligible presence of Fab′ fragments in systemic organs following pulmonary administration suggests the efficient clearance of the Fab′ fragments from the body, without significant systemic absorption. The high I^{125} signal found in the stomach following pulmonary and SC delivery of I^{125}-labeled Fab′ fragments might be due to in vivo catabolism of radioiodinated mAbs, release of iodotyrosine residues, deiodination of these residues and radioiodine uptake in the thyroid and stomach [33]. Sodium iodide symporter, an integral membrane protein, is expressed in thyroid epithelial cells and in the stomach and is responsible for iodine accumulation in these tissues [34]. While 12% of the delivered radioactive dose was found in the stomach following SC injection of Fab′ and pulmonary delivery of free I^{125}, this percentage increased to 15, 22 and 29% following pulmonary delivery of the anti-IL17A-PEG40, anti-IL-17A-PEG20 and anti-IL-17A, respectively. These larger quantities in the stomach as well as the detection of Fab′ fragments in nasal lavages might suggest that a fraction of the Fab′ fragments dose was cleared by mucocilliary clearance and then swallowed following pulmonary delivery. The rate of this clearance pathway appears to greatly decrease with PEG loading.

Taken together, our data indicate that conjugation of Fab′ fragments to PEG20 or PEG40 increases their residence time in both the healthy and inflamed lungs. Low systemic absorption of Fab′ fragments following pulmonary delivery prevents their accumulation in distant organs and thus reduces the probability of systemic side effects [6]. Reasons for the prolonged presence of PEGylated Fab′ in the airway lumen include binding to mucus, reduced cell uptake and reduced transport across lung epithelia. Fab′ fragments might be eliminated from the lungs by mucociliary clearance and then be swallowed and degraded in the gastrointestinal tract. Our results further show that SC injected Fab′ hardly penetrates into the lungs. This might imply that effective neutralization of cytokines in the lungs will require injection of high doses of Fab′ fragments. Further studies are warranted to find out the differences in efficacy between pulmonary administration and injection of anti-cytokine antibody fragments to reduce inflammation in the lungs.

Supplementary data to this article can be found online at https://doi.org/10.1016/j.jconrel.2017.12.009.

Acknowledgments

We thank Kevin Vanvarenberg for technical help. The anti-IL-13, anti-IL-13-PEG40 and anti-IL-17A Fab′ were kindly provided by UCB Pharma (Slough, United Kingdom). This work was supported by a research grant (grant number: T.0088.14) of the Fonds National de la Recherche Scientifique (FNRS, Belgium). Rita Vanbever is Maître de Recherches of the FNRS (Belgium).

The following are the supplementary data related to this article.

References

[1] B.N. Lambrecht, H. Hammad, The immunology of asthma, Nat. Immunol. 16 (2015) 45–56.
[2] L. Chini, E. Monteferrario, S. Graziani, V. Moschese, Novel treatments of asthma and allergic diseases, Paediatr. Respir. Rev. 15 (2014) 355–362.
[3] H.T. Tan, K. Sugita, C.A. Akdis, Novel biologicals for the treatment of allergic diseases and asthma, Curr. Allergy Asthma Rep. 16 (2016) 70.
[4] L. Guilleminault, N. Azzopardi, C. Arnoult, J. Sobilo, V. Herve, J. Montharu, A. Guillon, C. Andres, O. Herault, A. Le Pape, P. Diot, E. Lemarie, G. Paintaud, V. Gouilleux-Gruart, N. Heuze-Vourc'h, Fate of inhaled monoclonal antibodies after the deposition of aerosolized particles in the respiratory system, J. Control. Release 196 (2014) 344–354.
[5] W. Wang, E.Q. Wang, J.P. Balthasar, Monoclonal antibody pharmacokinetics and pharmacodynamics, Clin. Pharmacol. Ther. 84 (2008) 548–558.
[6] T.T. Hansel, H. Kropshofer, T. Singer, J.A. Mitchell, A.J. George, The safety and side effects of monoclonal antibodies, Nat. Rev. Drug Discov. 9 (2010) 325–338.
[7] J. Todoroff, R. Vanbever, Fate of nanomedicines in the lungs, Curr. Opin. Colloid Interface Sci. 16 (2011) 246–254.
[8] S.J. Koussoroplis, G. Paulissen, D. Tyteca, H. Goldansaz, J. Todoroff, C. Barilly, C. Uyttenhove, J. Van Snick, D. Cataldo, R. Vanbever, PEGylation of antibody fragments greatly increases their local residence time following delivery to the respiratory tract, J. Control. Release 187 (2014) 91–100.
[9] C. Loira-Pastoriza, J. Todoroff, R. Vanbever, Delivery strategies for sustained drug release in the lungs, Adv. Drug Deliv. Rev. 75 (2014) 81–91.
[10] H. Gursahani, J. Riggs-Sauthier, J. Pfeiffer, D. Lechuga-Ballesteros, C.S. Fishburn, Absorption of polyethylene glycol (PEG) polymers: the effect of PEG size on

permeability, J. Pharm. Sci. 98 (2009) 2847–2856.
[11] R.W. Niven, K.L. Whitcomb, L. Shaner, A.Y. Ip, O.B. Kinstler, The pulmonary absorption of aerosolized and intratracheally instilled rhG-CSF and monoPEGylated rhG-CSF, Pharm. Res. 12 (1995) 1343–1349.
[12] G. Pasut, F.M. Veronese, Polymer–drug conjugation, recent achievements and general strategies, Prog. Polym. Sci. 32 (2007) 933–961.
[13] A.P. Chapman, PEGylated antibodies and antibody fragments for improved therapy: a review, Adv. Drug Deliv. Rev. 54 (2002) 531–545.
[14] A. Minne, J. Louahed, S. Mehauden, B. Baras, J.C. Renauld, R. Vanbever, The delivery site of a monovalent influenza vaccine within the respiratory tract impacts on the immune response, Immunology 122 (2007) 316–325.
[15] P.L. Turecek, M.J. Bossard, F. Schoetens, I.A. Ivens, PEGylation of biopharmaceuticals: a review of chemistry and nonclinical safety information of approved drugs, J. Pharm. Sci. 105 (2016) 460–475.
[16] S. Heywood, Process for attaching effector molecules to proteins. Patent, 2007003898 A1 (2007).
[17] D. Freches, H.P. Patil, M. Machado Franco, C. Uyttenhove, S. Heywood, R. Vanbever, PEGylation prolongs the pulmonary retention of an anti-IL-17A Fab′ antibody fragment after pulmonary delivery in three different species, Int. J. Pharm. 521 (2017) 120–129.
[18] C.A. Fernandes, L. Fievez, B. Ucakar, A.M. Neyrinck, C. Fillee, F. Huaux, N.M. Delzenne, F. Bureau, R. Vanbever, Nicotinamide enhances apoptosis of G(M)-CSF-treated neutrophils and attenuates endotoxin-induced airway inflammation in mice, Am. J. Physiol. Lung Cell Mol. Physiol. 300 (2011) L354–361.
[19] J.L. Harcourt, L.M. Haynes, Establishing a liquid-covered culture of polarized human airway epithelial Calu-3 cells to study host cell response to respiratory pathogens in vitro, J. Vis. Exp. 72 (2013) 1–7.
[20] Y. Zhang, W.W. Reenstra, A. Chidekel, Antibacterial activity of apical surface fluid from the human airway cell line Calu-3: pharmacologic alteration by corticosteroids and beta(2)-agonists, Am. J. Respir. Cell Mol. Biol. 25 (2001) 196–202.
[21] M. Haghi, P.M. Young, D. Traini, R. Jaiswal, J. Gong, M. Bebawy, Time- and passage-dependent characteristics of a Calu-3 respiratory epithelial cell model, Drug Dev. Ind. Pharm. 36 (2010) 1207–1214.
[22] H.A. Farne, A. Wilson, C. Powell, L. Bax, S.J. Milan, Anti-IL5 therapies for asthma, Cochrane Database Syst. Rev. 9 (2017) CD010834.
[23] J.S. Patton, Mechanisms of macromolecule absorption by the lungs, Adv. Drug Deliv. Rev. 19 (1996) 3–36.
[24] W. Hofmann, B. Asgharian, The effect of lung structure on mucociliary clearance and particle retention in human and rat lungs, Toxicol. Sci. 73 (2003) 448–456.
[25] C. Lombry, D.A. Edwards, V. Preat, R. Vanbever, Alveolar macrophages are a primary barrier to pulmonary absorption of macromolecules, Am. J. Physiol. Lung Cell Mol. Physiol. 286 (2004) L1002–1008.
[26] W. Moller, K. Felten, K. Sommerer, G. Scheuch, G. Meyer, P. Meyer, K. Haussinger, W.G. Kreyling, Deposition, retention, and translocation of ultrafine particles from the central airways and lung periphery, Am. J. Respir. Crit. Care Med. 177 (2008) 426–432.
[27] M.M. Al-Tabakha, Future prospect of insulin inhalation for diabetic patients: the case of Afrezza versus Exubera, J. Control. Release 215 (2015) 25–38.
[28] V. Ghorani, M.H. Boskabady, M.R. Khazdair, M. Kianmeher, Experimental animal models for COPD: a methodological review, Tob. Induc. Dis. 15 (2017) 25.
[29] J.A. Regnis, M. Robinson, D.L. Bailey, P. Cook, P. Hooper, H.K. Chan, I. Gonda, G. Bautovich, P.T. Bye, Mucociliary clearance in patients with cystic fibrosis and in normal subjects, Am. J. Respir. Crit. Care Med. 150 (1994) 66–71.
[30] A. Patel, A. Woods, Y. Riffo-Vasquez, A. Babin-Morgan, M.C. Jones, S. Jones, K. Sunassee, S. Clark, T.M. De Rosales R, C. Page, D. Spina, B. Forbes, L.A. Dailey, Lung inflammation does not affect the clearance kinetics of lipid nanocapsules following pulmonary administration, J. Control. Release 235 (2016) 24–33.
[31] M.J. Guichard, T. Leal, R. Vanbever, PEGylation, an approach for improving the pulmonary delivery of biopharmaceuticals, Curr. Opin. Colloid Interface Sci. 31 (2017) 43–50.
[32] S.M. Kreda, S.F. Okada, C.A. van Heusden, W. O'Neal, S. Gabriel, L. Abdullah, C.W. Davis, R.C. Boucher, E.R. Lazarowski, Coordinated release of nucleotides and mucin from human airway epithelial Calu-3 cells, J. Physiol. 584 (2007) 245–259.
[33] S. Ram, D.J. Buchsbaum, Radioiodination of monoclonal antibodies D612 and 17-1A with 3-iodophenylisothiocyanate and their biodistribution in tumor-bearing nude mice, Cancer 73 (1994) 808–815.
[34] S. Filetti, J.M. Bidart, F. Arturi, B. Caillou, D. Russo, M. Schlumberger, Sodium/iodide symporter: a key transport system in thyroid cancer cell metabolism, Eur. J. Endocrinol. 141 (1999) 443–457.